Nonlinear prediction, filtering, and control of chemical systems from time series

Valery Petrov
Center for Nonlinear Dynamics, University of Texas, Austin, Texas 78712

Kenneth Showalter
Department of Chemistry, West Virginia University, Morgantown, West Virginia 26506-6045

(Received 9 April 1997; accepted for publication 23 June 1997)

Prediction, filtering and control of nonlinear systems is formulated in terms of corresponding nonlinear surfaces in the phase space of delayed system readings and control parameters. The construction of these surfaces from time series and their use is demonstrated with a simple chemical model in the chaotic regime. © *1997 American Institute of Physics.* [S1054-1500(97)00404-7]

Advances in controlling dynamical systems, stimulated in recent years by the challenge of chaotic dynamics, have been largely based on the development of linearized models from time series.[1] Linear control techniques for low-dimensional chaotic systems, such as the Ott–Grebogi–Yorke[2] method, have been successfully applied in a variety of physical, chemical, and biological settings.[3] Progress has also been made in the development of linear methods for controlling high-dimensional systems.[4–7] Nonlinear techniques, where measurements and perturbations are not restricted to a linear region around the state of interest, are less well developed. We present a unified approach for nonlinear prediction, filtering and control based on the construction of appropriate nonlinear hypersurfaces directly from time-series readings. A three-variable model for chemical chaos is used to demonstrate the approach, which permits global characterization and control of dynamical behavior without knowing the underlying mechanistic features or governing equations of the dynamical system.

I. INTRODUCTION

The prediction of the future behavior of dynamical systems is a broadly discussed topic due to the many possibilities for practical applications. We consider the problem of time-series prediction as an introduction to our method of nonlinear surface reconstruction. The technique is demonstrated by constructing the prediction surface from a chaotic time series and then using this surface to predict future behavior.

Nonlinear filtering allows the reconstruction of one system observable from delayed readings of a second system observable. In our chemical model, the system observables are related to the concentrations of the chemical species of the reaction. The concentration of one component might be measured, for example, by monitoring the system with an ion-selective electrode. This signal can then be used to calculate the precise concentration of another component of the reaction at any time, even when the reaction is in the chaotic regime and the system trajectory is nonrepeating.

Nonlinear control provides the means to direct the trajectory of a system to a desired goal in phase space. The goal is typically an unstable steady or periodic state, which, once it is realized, is then stabilized by the algorithm. The control objective or goal can also be some dynamical pattern not found in the autonomous system. In each case, the control objective is approached in a minimum number of steps by the algorithm.

II. PREDICTION

Prediction of the future evolution of a multidimensional system is closely related to the ability to reconstruct the system state from available observations. The evolution of the system can then be described in terms of the coordinates along the system manifolds. When the trajectory is sampled at even time intervals, the readings of the coordinates at each iteration represent the state of the system at that iteration.

Consider a general two-dimensional nonlinear system, where (ξ, η) are the coordinates along the system manifolds. The manifolds originating from the eigenvectors of a particular steady state are shown schematically in Figure 1. We first consider only a small region around the steady state where a linear description can be used to characterize the time evolution of the discretized system:

$$\xi_{i+1}=\lambda_{\xi}\xi_i, \quad \eta_{i+1}=\lambda_{\eta}\eta_i. \tag{1}$$

Here, ξ_i, η_i are the components of the vector defining the tip of the system trajectory in phase space, λ_{ξ}, λ_{η} are the eigenvalues along the corresponding eigenvectors, and $(\xi, \eta)=(0, 0)$ are the coordinates of the steady state. Usually the behavior of the system variables cannot be observed directly but, rather, is projected on some variable x, which we denote the observable variable:

$$x_i=t_{\xi}\xi_i+t_{\eta}\eta_i, \tag{2}$$

where t_{ξ} and t_{η} are the projection coefficients. In a chemical system, x is typically a physical observable related to the concentrations of the component species. Since x_{i+1} is given by Eq. (2) for iteration $i+1$ and Eq. (1) determines the position of the (ξ_{i+1}, η_{i+1}) state from the (ξ_i, η_i) state, knowing (ξ_i, η_i) is sufficient to predict x_{i+1} provided that the time-independent system parameters are known. Hence,

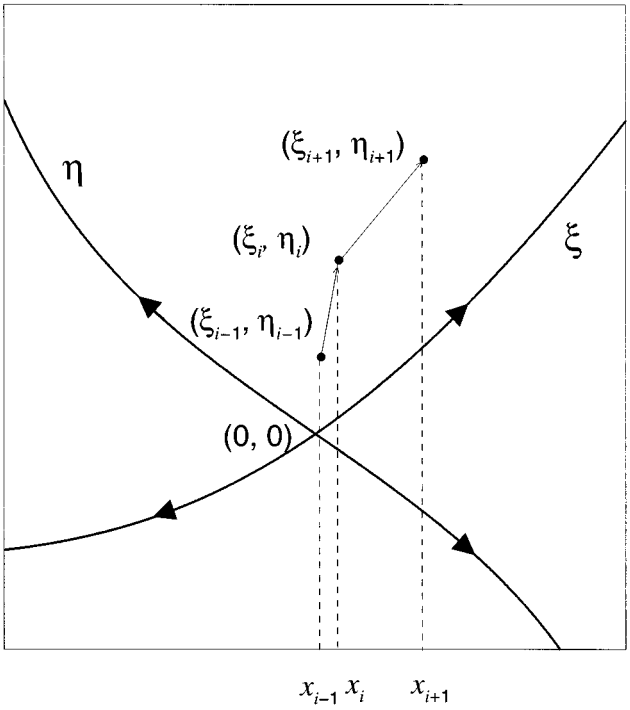

FIG. 1. Schematic representation of the nonlinear manifolds of a general two-variable system. The state of the system (ξ_i, η_i) is not observed directly; however, it can be reconstructed from consecutive readings of observable x as the system evolves from the previous state (ξ_{i-1}, η_{i-1}). As a result, the future state (ξ_{i+1}, η_{i+1}) and the corresponding observable x_{i+1} can be predicted from the observations of x_i and x_{i-1}.

$$x_{i+1} = \Pi(\xi_i, \eta_i), \tag{3}$$

where Π is a linear function and $(\xi_i,\ \eta_i)$ can be found from the measurement of two independent observables at iteration i. If we have fewer independent observables than the number of internal degrees of freedom, the prediction is still possible using time-delayed readings of the available observables.[8,9] For a single observable x in the two-dimensional case, Eqs. (1) and (2) for iteration $i-1$ give

$$x_{i-1} = \lambda_\xi^{-1} t_\xi \xi_i + \lambda_\eta^{-1} t_\eta \eta_i . \tag{4}$$

Equations (2) and (4) can be solved to express $(\xi_i,\ \eta_i)$ in terms of $(x_i,\ x_{i-1})$,

$$\begin{pmatrix} \xi_i \\ \eta_i \end{pmatrix} = \vec{L}(x_i, x_{i-1}), \tag{5}$$

where $\vec{L}$ is a linear function of its arguments. From Eqs. (3) and (5), we can now express the observable at iteration $i+1$,

$$x_{i+1} = P(x_i, x_{i-1}), \tag{6}$$

where P is a linear function that allows prediction of the system evolution based on the previous readings.

Equation (6) is valid only for a two-variable linear system. An analogous equation can be derived, however, for a linear m-dimensional system, where Eq. (6) is modified by the additional terms $x_{i-2}, x_{i-3}, \ldots, x_{i-m+1}$. Furthermore, if the dynamics of the system is governed by nonlinear equations of motion, the function P is linear only in a small neighborhood of the steady state where the linear approximation is valid. As the range is increased into the nonlinear regime, we expect P to become a nonlinear mapping. In a highly nonlinear regime, more than two delayed readings may be necessary to correctly predict the behavior in a single-valued fashion[9] due to twisting of the manifolds. For a multidimensional system with an unknown dimensionality, the following form for the mapping is assumed:

$$x_{i+1} = \mathbf{P}(x_i, x_{i-1}, \ldots, x_{i-m+1}), \tag{7}$$

where m is the dimensionality of the embedding space. This form is well known from time-series prediction theory;[1] however, we have taken a somewhat different approach in our development that will prove to be useful in the subsequent development of nonlinear filtering and control. The function $\mathbf{P}$ can be thought of as a nonlinear hypersurface in the phase space of delayed variables. Several techniques can be used to estimate $\mathbf{P}$ and m from time series when the exact equations governing the dynamics are not known.

To illustrate the implementation of the prediction technique we consider a model for chemical chaos,[10] which is a three-variable version of the autocatalator model:[11]

$$\begin{aligned} d\alpha/d\tau &= \mu(\kappa+\gamma) - \alpha\beta^2 - \alpha, \\ \sigma d\beta/d\tau &= \alpha\beta^2 + \alpha - \beta, \\ \delta d\gamma/d\tau &= \beta - \gamma. \end{aligned} \tag{8}$$

Here, α, β, and γ are dimensionless concentrations and σ, δ, μ, and κ are the dimensionless parameters of the model. For $\sigma=0.015$, $\delta=1$, $\mu=0.301$, and $\kappa=2.5$, the behavior is chaotic with each of the concentrations exhibiting highly nonlinear behavior.[12] We use Eqs. (8) only to generate time series of the variable α, which we transform to $\log(\alpha)$ to simulate a realistic measurement of the concentration by an ion-selective electrode. Thus, we construct the nonlinear function $\mathbf{P}$ using the ''observable'' $\log(\alpha)$ from a reference set of 8000 data points generated by the model. The validation of the prediction model—i.e., the comparison of the predicted behavior with the ''true'' dynamics—is carried out using data generated directly from Eqs. (8).

A local linear regression method[13] was used for the interpolation of $\mathbf{P}$ in phase space, where, assuming $\mathbf{P}$ is a differentiable surface, we draw the tangential plane to the surface at any point to provide a first-order approximation of the neighborhood of that point. A set of tangential planes drawn at a number of grid points in phase space can therefore be used as a first-order approximation of the entire surface $\mathbf{P}$. The storage of the surface parameters at all selected grid points may require a prohibitively large amount of data if the dimensionality of the embedding space is large; we therefore retain the reference data set in order to approximate the surface at any point when it is required by the algorithm. Thus, to approximate the function $\mathbf{P}$ at some point $\mathbf{x}=(x_i, \ldots, x_{i-m+1})$ we find the k points from the reference data set closest to $\mathbf{x}$. This requires a sorting routine to be carried out on the reference data set every time we want to use $\mathbf{P}$ to make a prediction. The nearest neighbors found in the sorting are then used for approximating the surface at the

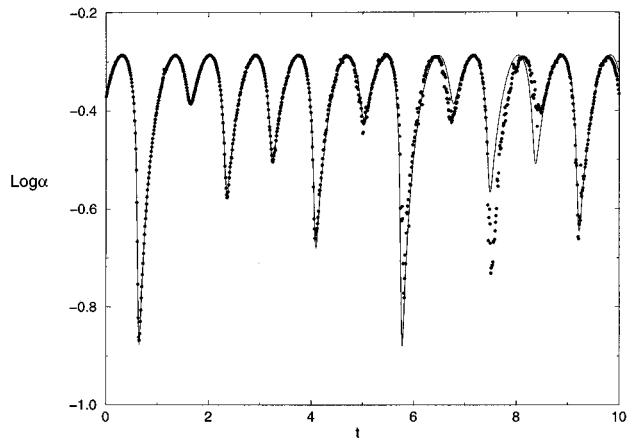

FIG. 2. Prediction of a chaotic time series of the three-variable autocatalator, Eqs. (8). The prediction nonlinear surface **P** was approximated from an earlier recorded data set by using a local linear interpolation with 12 nearest points.

point of interest, and, once the parameters of the plane are determined, x_{i+1} is calculated from **x** via Eq. (7). In the absence of noise, m points are sufficient to draw a hyperplane in m-dimensional space. If noise is present, it is desirable to have more data points and use a least-squares fitting procedure to determine the parameters of the plane. On the over-determined data set of the present example, we used the robust technique of singular-value decomposition[14] to find the approximating plane.

The optimal number of neighbors k depends on the nonlinearity of the surface and density of points in the region of phase space where the approximation is made. Although a larger neighborhood allows more points to be used in calculating the approximation, it may be best to use a smaller neighborhood in regions with high local curvature, since the remote points may introduce a systematic error due to the deviation of the surface from the plane. The optimal approximation should therefore take into account different curvatures of the surface in different regions of phase space. Here, we use the simplified approach of selecting a constant number of approximating neighbors throughout phase space. Calculating the prediction error as the standard deviation of the predicted signal from the original time series as a function of different numbers of approximating neighbors, we found that $k=3m$ gave the lowest error for this example. This particular choice depends not only on the curvature of the **P** surface but also on the number of reference points used in the approximating data set. Our choice of 8000 points was based on the assumption that 10^m points are necessary for a reasonable representation of the m-dimensional surface using an equally distributed mesh of points with 10 points per dimension. The prediction error decreases as the overall number of the data points increases; however, the computational and storage requirements place an upper limit on the number of points that can be used in defining the prediction surface.

Figure 2 shows an application of the prediction technique for a chaotic time series of the autocatalator model, Eqs. (8). The prediction begins at $t = 0.0$ and relies only on information stored for $t<0$. Equation (7) is used in the following form:

$$x(t_p)=\mathbf{P}(x(0),x(-\tau),x(-2\tau),x(-3\tau)), \tag{9}$$

where $x=\log(\alpha)$, $\tau=0.8$, and $0<t_p<10$. Equation (9) is expressed in terms of four time-delay coordinates, giving a dimension that was found to produce the smallest prediction error. This is consistent with an estimation of the embedding dimension from the fractal dimension,[15] $D=2n-1$, which should be between 4 and 5 since the dimension of the attractor is known to be greater than 2 but less than 3.[10] A small amount of Gaussian noise (60 db signal-to-noise ratio) was also added to the time series. A divergence of the predicted behavior from the ''true'' behavior is observed in Fig. 2 for $t>7$, which is anticipated with the presence of a positive Lyapunov exponent.

One can also define the nonlinear hypersurface using artificial neural networks. We found, however, that the local linear approximation results in a smaller prediction error than a feed-forward neural network with up to 100 sigmoidal neurons.[16]

III. FILTERING

We now assume there is another observable that is also a projection of the system dynamics but with a different set of projection coefficients. For our general two-dimensional system, the second observable y is given by

$$y_i=r_\xi\xi_i+r_\eta\eta_i, \tag{10}$$

where r_ξ and r_η are the projection coefficients. By combining Eqs. (5) and (10), y_i can be expressed as a function of delayed readings of x,

$$y_i=F(x_i,x_{i-1}), \tag{11}$$

where F is a linear function. Equation (11) is known as a finite impulse response (FIR) filter, where the filtered signal y depends only on a finite length of the signal x. For nonlinear multidimensional systems, we expand Eq. (11) to

$$y_i=\mathbf{F}(x_i,x_{i-1},\ldots,x_{i-m+1}), \tag{12}$$

where **F** is a nonlinear function of its arguments and can be thought of as a high-dimensional surface in $(y_i, x_i,\ldots,x_{i-m+1})$ space. We can therefore establish a direct relation between different observable variables of a nonlinear system, since these variables represent projections from the same manifolds of the system.

We demonstrate the filtering method by constructing the **F** surface with 8000 data points generated from the autocatalator model in the chaotic regime. The construction of **F** requires the time series of two observables: we choose $x=\log(\alpha)$ and $y=\log(\beta)$ to simulate a chemical system monitored with two ion-specific electrodes. Once the surface is available, the behavior of y at any time can be found from the corresponding time series of x, even for chaotic behavior where the trajectory in phase space never exactly repeats itself. Figure 3 shows the prediction of $y=\log(\beta)$ from an

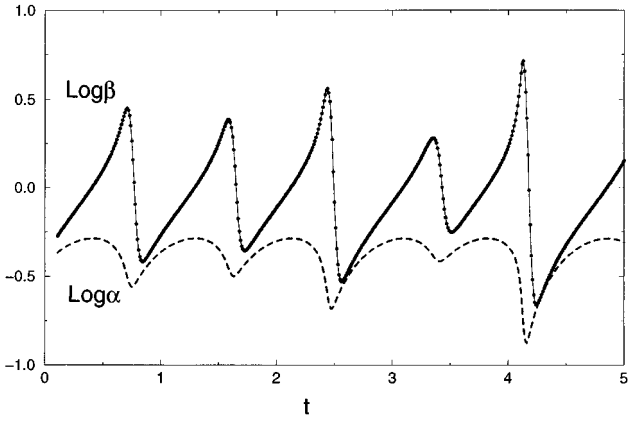

FIG. 3. Filtering output from a chaotic time series of the autocatalator, Eqs. (8). Solid line shows the ''true'' value of $\log(\beta)$; dots show output of filter designed to approximate $\log(\beta)$ at selected time intervals. Dashed line shows the value of $\log(\alpha)$, the input of the nonlinear filter. The filtering surface **F** (of dimension 5) was constructed from the previously collected data points from time series of $\log(\alpha)$ and $\log(\beta)$.

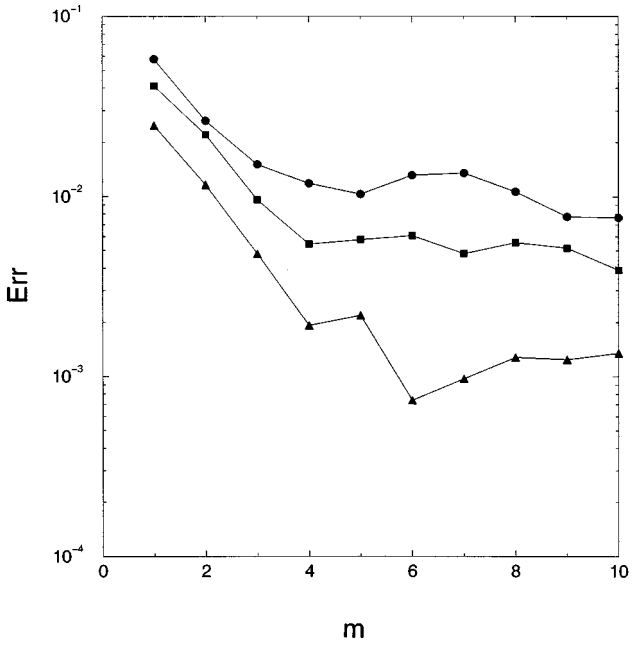

FIG. 4. Error of the filtered signal $\log(\beta)$ predicted from $\log(\alpha)$ compared to the ''true'' $\log(\beta)$ as a function of the assumed dimension m and the number of reference points used to approximate the filtering surface **F**. The series of dots corresponds to 1000 reference points, the squares to 3000 points, and the triangles to 10 000 points used to approximate **F**.

arbitrary time series of $x=\log(\alpha)$. We see that the filtered values of $\log(\beta)$ correspond to the ''true'' values with a very good accuracy.

In general, the embedding dimension used in Eq. (12) is not known; however, it can be determined during the construction of **F** when y is available by measuring the filtering error for different values of m. The optimal dimension is selected by determining the value above which the error is not significantly decreased. This value of m does not necessarily reflect the actual embedding dimension of the system, but, rather, the embedding dimension that gives the best reconstruction of **F**. As shown in Figure 4, m depends on other factors, including the level of noise present in the time series as well as the number of data points used in the surface construction.

Even though the time series of both the x and y variables are required during the construction stage, the nonlinear filter can be very useful when the second variable y is difficult to obtain. Thus, it is necessary to measure y together with x in only one experiment; the filter can then be used to generate y whenever this observable might be difficult or impossible to measure. Unlike the linear filter, Eq. (12) allows the extraction of signals that have similar fundamental frequencies and that are mixed together in a nonlinear fashion.

The mixture of signals generated by deterministic nonlinear systems results in an effectively new dynamical system, but each signal can also be thought of as a nonlinear projection of the internal dynamics of the corresponding subsystem. This concept is demonstrated in Fig. 5, where a saw-tooth signal is filtered out of a nonlinear mixing of this signal with a chaotic time series from the autocatalator model, log (α). The filtered signal is in good agreement with the ''true'' signal of the saw-tooth subsystem, although the error is slightly larger than in the previous example shown in Fig. 3. The dynamics of the mixed system corresponds to the combination of the independent nonlinear systems and, consequently, the optimal embedding dimension in Eq. (12) increased to a value of 9.[17]

IV. CONTROL

The concept of constructing a nonlinear surface from time series can also be used in the control of nonlinear dynamical systems.[18] Control assumes the availability of a system parameter p to which perturbations can be applied to alter the system dynamics. We again consider a general two-dimensional linear system for our development. To move the system from the current state $(\xi_i,\ \eta_i)$ to a given target state (ξ_{i+2},η_{i+2}), a sequence of two control perturbations is required.[5] Since the sequence of perturbations is unique for a given pair of current and target states, we can write a control equation for the first perturbation of the sequence in terms of these states:

$$p_{i+1}=\Xi\left(\begin{pmatrix}\xi_i\\ \eta_i\end{pmatrix},\begin{pmatrix}\xi_{i+2}\\ \eta_{i+2}\end{pmatrix}\right), \tag{13}$$

where Ξ is a linear function. Even though a sequence of two perturbations must be applied before the desired state is reached, it is necessary to explicitly determine only the first perturbation since the second perturbation can be calculated at the next iteration using the same expression with the updated readings.

We now consider defining the system state in a manner analogous to Eq. (5) in order to obtain a general expression for the control perturbations in terms of the delayed observations. There are two complications, however, that prevent us from using Eq. (5) directly. First, the control perturbations

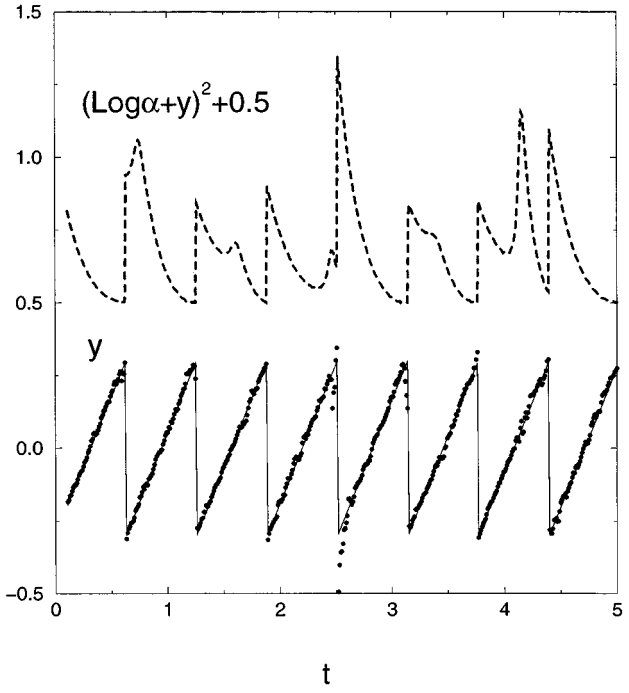

FIG. 5. Filtering output of a saw-tooth signal (dots) from the filter input (dashed line) given by $(\log(\alpha)+y)^2+0.5$, where y represents a saw-tooth function with an amplitude of 0.3 and $\log(\alpha)$ is a chaotic signal from Eqs. (8). The ''true'' saw-tooth signal is shown by the solid line. An embedding dimension of 9 was selected for the nonlinear filter surface **F**.

applied to the system shift the vector field in phase space and therefore introduce an additional variable that must be included in the description. Second, it is not possible to express the target state in Eq. (13) in terms of delayed readings since these readings will depend upon the control perturbations applied during the transition sequence. To avoid this complication, we will define the target state in terms of the time-forwarded sequence.

Consider the system trajectory in the linear neighborhood of a fixed point. If a perturbation is applied to the system at iteration i and maintained constant and equal to p_{i+1} during one sampling period, the system state at iteration $i+1$ is given by

$$\begin{aligned} \xi_{i+1} &= \lambda_\xi \xi_i + (1-\lambda_\xi)\alpha_\xi\, p_{i+1}, \\ \eta_{i+1} &= \lambda_\eta \eta_i + (1-\lambda_\eta)\alpha_\eta\, p_{i+1}, \end{aligned} \tag{14}$$

where $\alpha_\xi = \partial \xi_s / \partial p$ and $\alpha_\eta = \partial \eta_s / \partial p$ give the shift of the steady state in the ξ and η directions due to the perturbation.[5] Equation (14), together with equations for the observable x at iterations i and $i+1$,

$$\begin{aligned} x_i &= t_\xi \xi_i + t_\eta \eta_i, \\ x_{i+1} &= t_\xi \xi_{i+1} + t_\eta \eta_{i+1}, \end{aligned} \tag{15}$$

are sufficient to solve for $(\xi_i,\ \eta_i)$ in terms of the time-forwarded readings and applied perturbations:

$$\begin{pmatrix} \xi_i \\ \eta_i \end{pmatrix} = \vec{N}(x_i, x_{i+1}, p_{i+1}), \tag{16}$$

where $\vec{N}$ is a linear function. In addition, Eqs. (14) and (15) can be solved for the state (ξ_{i+1}, η_{i+1}):

$$\begin{pmatrix} \xi_{i+1} \\ \eta_{i+1} \end{pmatrix} = \vec{M}(x_{i+1}, x_i, p_{i+1}), \tag{17}$$

where $\vec{M}$ is another linear function. Shifting the index in Eq. (17) from $i+1$ to i yields

$$\begin{pmatrix} \xi_i \\ \eta_i \end{pmatrix} = \vec{M}(x_i, x_{i-1}, p_i). \tag{18}$$

The system state $(\xi_i,\ \eta_i)$ in Eq. (16) and Eq. (18) is expressed in terms of time-forwarded and time-delayed readings and perturbations. Shifting the index from i to $i+2$ in Eq. (16) and substituting this, together with Eq. (18), into Eq. (13) yields a control law of the form

$$p_{i+1} = C(x_i, x_{i-1}, p_i, x_{i+2}, x_{i+3}, p_{i+3}), \tag{19}$$

where C is a linear control function. Notice that the control perturbation p_{i+1} depends only on the readings and perturbations that occur before p_{i+1} is applied and after the control sequence p_{i+1}, p_{i+2} is complete. This allows us to define the target state in terms of the desired values of the observable at the end of the control sequence. The stabilization of an unstable steady state, for example, should result in the dynamics observed at this state in the absence of the external perturbations; the desired state is therefore $x_{i+2} = x_{i+3} = x_{steady\ state}$ and the perturbation $p_{i+3} = 0$.

For an m-dimensional nonlinear system, Eq. (19) can be generalized to

$$\begin{aligned} p_{i+1} = \mathbf{C}(&x_i, x_{i-1}, \ldots, x_{i-m+1}; p_i, p_{i-1}, \ldots, p_{i-m+2}; \\ &x_{i+m}, \ldots, x_{i+2m-1}; p_{i+m+1}, \ldots, p_{i+2m-1}), \end{aligned} \tag{20}$$

where **C** is a nonlinear surface in the extended space that includes time-delayed and time-forwarded perturbations and observations. The complexity of Eq. (20) does not prevent it from being robust in the implementation of control. It is not even necessary to know the exact position of the steady state if Eq. (20) is rearranged to express the target state in terms of differences of the observable at subsequent iterations.[18] The control law then takes the form

$$\begin{aligned} p_{i+1} = \mathbf{S}(&x_i, x_{i-1}, \ldots, x_{i-m+1}; p_i, p_{i-1}, \ldots, p_{i-m+2}; \\ &(x_{i+m+1} - x_{i+m}), \ldots, (x_{i+2m} - x_{i+2m-1}); \\ &p_{i+m+1}, \ldots, p_{i+2m}), \end{aligned} \tag{21}$$

where **S** is a nonlinear function formulated specifically for steady state stabilization.

Figure 6 shows an application of the method to stabilize the unstable steady state and thereby suppress chaotic behavior in the autocatalator, where perturbations to the system parameter μ in Eqs. (8) were calculated from Eq. (21). To approximate the **S** surface, 1000 random perturbations were applied to the parameter μ and the system responses were collected. The process of stabilization was then carried out by substituting the m delayed readings and $m-1$ delayed perturbations, which define the current state, into the first set

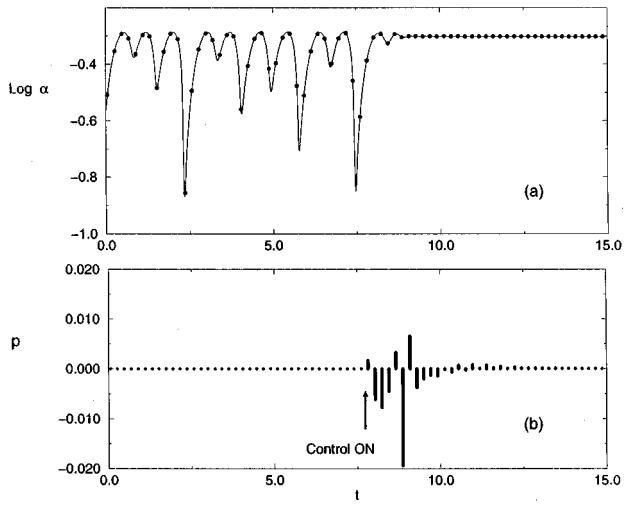

FIG. 6. Suppression of chaotic behavior and stabilization of the unstable steady state of Eqs. (8) using the control surface **S**. (a) Time evolution of $\log(\alpha)$ shown by the solid line; intervals when the system was sampled shown by dots. (b) Sequence of perturbations for controlling the system. The perturbation sequence was started at $t = 7.8$. Each perturbation, which is kept constant for the duration of the sampling interval, was calculated from the **S** surface using the previous 4 readings of $\log(\alpha)$ and the previous 3 perturbations. After $t = 13$, the system resides very close to the stationary state and only very small perturbations are necessary to maintain the system at this state.

of terms of the **S** function [upper line of Eq. (21)]. The desired behavior of the target state yields zeros for the second set of terms in **S** [lower line in Eq. (21)]. With these substitutions, the **S** function returns the first control perturbation. The second control perturbation is returned on the next iteration, and so on. After completion of the m-perturbation cycle, the system will reside very close to the objective state. Figure 6(a) shows a time series of the stabilization procedure, where the sampling intervals of the system are indicated by the dots. The corresponding sequence of perturbations is shown in Fig. 6(b). For this example, the fastest convergence was found to occur with $m=4$. A nonideal convergence of the algorithm was observed due to the relative scarcity of data points in the 16-dimensional embedding space of the **S** surface.

The same algorithm has been successfully applied in the control of convective instabilities in a liquid bridge experiment.[19] The control function for the four-dimensional dynamics was reconstructed from 500 data points, allowing the stabilization of periodic behavior in the quasiperiodic regime.

V. CONCLUSION

We have presented algorithms for nonlinear prediction, filtering and control based on the construction of appropriate invariant functions directly from time series. Our approach has been first to demonstrate the construction of a linear invariant function based on time-series measurements in the linear regime. We then assume, based on arguments of functional continuity, that the invariant function can be extended into nonlinear regimes. The appropriate nonlinear function allows the prediction of future behavior, defines functional relations between evolving system variables (or the related system observables), or permits dynamic control of behavior by parameter perturbations.

The nonlinear filtering method could be particularly effective in situations where two signals are mixed with approximately the same frequencies but different types of nonlinearities. Consider, for example, the extraction of the heartbeat signal of a fetus from the EKG of the mother.[20] The **F** surface might first be constructed from the EKG of the mother and ultrasound measurements of the fetus heartbeat. During subsequent checkups, only the EKG of the mother would be required since the heartbeat of the fetus could be simply filtered out of this signal. Of course, this approach would be strictly applicable only if the general nature of the heartbeats of the mother and fetus did not change over time. The changing period and amplitude of the heartbeat of the fetus as it matures would undoubtedly diminish the precision of the technique. One possible approach might be to construct an **F** surface based on the signals from a pool of patients for each month of pregnancy.

The nonlinear control algorithm can be used for selective switching between remote coexisting states of nonlinear dynamical systems. For example, two bistable reactions carried out in coupled reactors may exhibit four different stable steady states.[21] A single parameter, such as the coupling strength or reactor residence time, could be used to move the system between any of these four states.

The fact that prediction, filtering and control can be formulated from previously observed responses in terms of a surface—or, effectively, a look-up table—suggests that all of these tasks could be carried out in a similar manner by neuronal networks of living systems.

ACKNOWLEDGMENTS

We thank E. Mihaliuk and H. Sun for valuable discussions and the National Science Foundation (CHE-9531515), the Office of Naval Research (N00014-95-1-0247), and the Petroleum Research Fund (29565-AC6) for supporting this research.

[1] H. D. I. Abarbanel, R. Brown, J. J. Sidorowich, and L. S. Tsimring, ''The analysis of chaotic data in physical systems,'' Rev. Mod. Phys. **65**, 1331 (1993).
[2] E. Ott, C. Grebogi, and J. A. Yorke, ''Controlling chaos,'' Phys. Rev. Lett. **64**, 1196 (1990).
[3] For recent reviews, see: T. Shinbrot, C. Grebogi, E. Ott, and J. A. Yorke, ''Using small perturbations to control chaos,'' Nature (London) **363**, 411 (1993); W. L. Ditto and L. Pecora, ''Mastering chaos,'' Sci. Am. **269**, 78 (1993); E. Ott and M. Spano, ''Controlling chaos,'' Phys. Today **48**, 34 (1995).
[4] P. So and E. Ott, ''Controlling chaos using time delay coordinates via stabilization of periodic orbits,'' Phys. Rev. E **51**, 2955 (1995).
[5] V. Petrov, E. Mihaliuk, S. K. Scott, and K. Showalter, ''Stabilizing and characterizing unstable states in high dimensional systems from time series,'' Phys. Rev. E **51**, 3988 (1995).
[6] V. Petrov, S. Metens, P. Borckmans, G. Dewel, and K. Showalter, ''Tracking unstable turing patterns through mixed-mode spatiotemporal chaos,'' Phys. Rev. Lett. **75**, 2895 (1995).
[7] M. Ding, W. Yang, V. In, W. L. Ditto, M. L. Spano, and B. Gluckman,

''Controlling chaos in high dimensions: Theory and experiment,'' Phys. Rev. E **53**, 4334 (1996).
[8] N. H. Packard, J. P. Crutchfield, J. D. Farmer, and R. S. Shaw, ''Geometry from a time series,'' Phys. Rev. Lett. **45**, 712 (1980).
[9] F. Takens, ''Detecting strange attractors in turbulence,'' in *Dynamical Systems and Turbulence*, edited by D. A. Rand and L.-S. Young, Springer Lecture Notes in Mathematics (Springer-Verlag, New York, 1980), Vol. 898, pp. 366–381.
[10] B. Peng, S. K. Scott, and K. Showalter, ''Period doubling and chaos in a three-variable autocatalator,'' J. Phys. Chem. **94**, 5243 (1990).
[11] P. Gray and S. K. Scott, ''Autocatalytic reactions in the isothermal, continuous stirred tank reactor. Oscillations and instabilities in the system $A+2B\rightarrow 3B$, $B\rightarrow C$,'' Chem. Eng. Sci. **39**, 1087 (1984).
[12] V. Petrov, S. K. Scott, and K. Showalter, ''Mixed-mode oscillations in chemical systems,'' J. Chem. Phys. **97**, 6191 (1992).
[13] R. Cawley and G.-H. Hsu, ''Local-geometric-projection method for noise reduction in chaotic maps and flows,'' Phys. Rev. A **46**, 3057 (1992).
[14] W. H. Press, S. A. Teukolsky, W. T. Vetterling, and B. P. Flannery, *Numerical Recipes in C*, 2nd ed. (Cambridge University Press, Cambridge, 1992).
[15] J. D. Farmer, E. Ott, and J. A. Yorke, ''The dimension of chaotic attractors,'' Physica D **7**, 153 (1983).
[16] Time-delayed readings of the observable were supplied to an input layer consisting of four linear neurons. The second layer consisted of 100 sigmoidal neurons and the third, output layer consisted of one linear neuron. The network was trained using back-propagation and then applied for the time-series prediction.
[17] The number of points used in the reconstruction of **F** was the same for Figs. 3 and 5.
[18] V. Petrov and K. Showalter, ''Nonlinear control of dynamical systems from time series,'' Phys. Rev. Lett. **76**, 3312 (1996).
[19] V. Petrov, M. F. Schatz, K. A. Muehlner, S. J. VanHook, W. D. McCormick, J. B. Swift, and H. L. Swinney, ''Nonlinear control of remote unstable states in a liquid bridge experiment,'' Phys. Rev. Lett. **77**, 3779 (1996).
[20] T. Schreiber and D. Kaplan, ''Signal separation by nonlinear projections: The fetal electrocardiogram,'' Phys. Rev. E **53**, R4326 (1996).
[21] K. L. C. Hunt, J. Kottalam, M. D. Hatlee, and J. Ross, ''Multiple steady states in coupled flow tank reactors,'' J. Chem. Phys. **96**, 7019 (1992).